

Experimental Observation of Superparamagnetism in Manganese Clusters

Mark B. Knickelbein

Chemistry Division, Argonne National Laboratory, Argonne, Illinois 60439

(Received 29 January 2001)

A molecular beam of manganese clusters, Mn_n ($n = 11-99$), produced at 68 K is deflected toward high field by a gradient field magnet. These results indicate that Mn_n clusters in this size range are superparamagnetic species whose intrinsic moments can be determined within the framework of the Langevin model of paramagnetism. Local minima in per-atom magnetic moments are observed for Mn_{13} and Mn_{19} , suggestive of an icosahedral growth sequence for the smaller size range. For larger clusters, broad oscillations in the per-atom moments are observed, with a minimum near Mn_{32-37} and a maximum around Mn_{50-56} .

DOI: 10.1103/PhysRevLett.86.5255

PACS numbers: 36.40.Cg, 39.10.+j, 82.80.Rt

The search for magnetic behavior in nonferromagnetic transition metals has often focused on the effects of reduced dimension. Atomic clusters represent an important class of reduced dimensionality systems and have produced some unexpected results bearing on magnetic ordering in small systems. For example, molecular beam magnetic deflection experiments performed by Bloomfield and co-workers showed that rhodium clusters (Rh_{9-60}) display nonzero magnetic moments [1,2] indicative of ferromagnetic ordering, even though bulk rhodium is nonmagnetic [3]. Surveys by the Virginia group aimed at searching for other cases of “anomalous” magnetic ordering in clusters composed of nonferromagnetic transition metals, specifically V_n , Ru_n , and Pd_n , failed to reveal other such examples [2,4]. However, recently this group has observed nonzero magnetic moments indicative of ferromagnetic ordering in chromium clusters [5].

In this Letter, we present the results of magnetic deflection experiments that show that manganese clusters in the size range $Mn_{11}-Mn_{99}$ display nonzero magnetic moments indicative of ferromagnetic ordering of spins, despite the fact that no known bulk phase of Mn displays such ordering [3]. These findings are in accord with recent theoretical studies predicting ferromagnetic ordering in small manganese clusters [6,7]. ESR studies by Weltner and co-workers have shown that matrix-isolated Mn_2 is antiferromagnetically coupled, whereas Mn_5 is a high-spin molecule with $S = \frac{25}{2}$ resulting from ferromagnetic coupling of spins [8,9]. The magnetic behavior of a somewhat different type of manganese clusters has attracted considerable attention recently [10–13]. In particular, low temperature magnetization measurements of oriented crystals of $Mn_{12}O_{12}(CH_3COO)_{16}(H_2O)_4$ (“ Mn_{12} acetate”) produced hysteresis loops having discrete steps [10]. In Mn_{12} acetate molecules, four Mn^{4+} ions ($S = \frac{3}{2}$) and eight Mn^{3+} ions ($S = 2$) couple to produce a ferrimagnetic high-spin molecule with $S = 10$. The emergence of steps in the magnetization curves is a result of resonant tunneling between spin states, facilitated by the magnetocrystalline anisotropy of the sample. The results reported in this Letter show that

neutral, bare manganese clusters can also be considered high-spin molecules.

The apparatus consists of a three-stage molecular beam machine incorporating a gradient dipole (i.e., Stern-Gerlach-type) magnet. Manganese clusters were produced within a continuous-flow laser vaporization source coupled to a high aspect ratio flow tube (9 cm length \times 0.3 cm diam) held at 68 ± 2 K [14]. The residence time within the flow tube (~ 1 ms) was sufficient to ensure that the clusters were equilibrated to the flow tube temperature prior to expansion into vacuum. At the helium flow rates used, the pressure within the flow tube was 10 ± 1 Torr. The clusters expanded into vacuum through a 1.0 mm diam orifice at the end of the flow tube. Under these mild expansion conditions, very little supersonic cooling of the clusters’ vibronic degrees of freedom is expected [15], so that the postexpansion cluster temperature is estimated to be close (within ~ 5 K) to that of the flow tube. The expanding jet was skimmed into a molecular beam, which passed through a Stern-Gerlach-type gradient magnet [16] capable of producing B fields of up to ~ 1.2 T and gradients ($\partial B/\partial z$) up to ~ 210 Tm $^{-1}$ in the center of the gap. The clusters were detected via position-sensitive time-of-flight (PSTOF) mass spectrometry [17] 0.9 m downbeam of the magnet, from which the spatial deflections of the clusters were determined. The magnetization ($\langle M_z \rangle$) of the clusters were calculated from the magnitude of the deflection (as computed from the change in TOF mass peak first moments), the molecular beam speed, B and $\partial B/\partial z$, and the apparatus dimensions as described by others [18,19]. A full description of the experimental apparatus and methods will be provided in a future publication [20].

A magnified portion of the TOF spectrum, showing traces recorded with the deflection field off vs on, is shown in Fig. 1. The temporal width of the TOF peaks in the field-off trace reflects the natural width of the molecular beam (~ 2 mm) as measured by time domain position-sensitive detection [17]. The shift of the Mn_n TOF peaks to later arrival times in the field-on trace

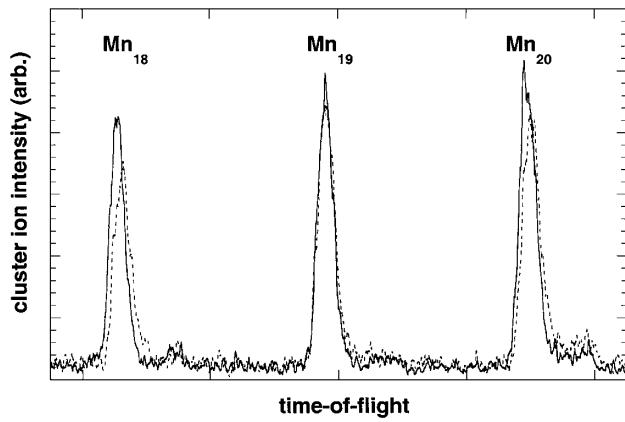


FIG. 1. A magnified view of the manganese cluster time-of-flight spectrum showing Mn₁₈–Mn₂₀. Solid trace: $B = 0$; dashed trace: $B = 0.97$ T, $\partial B/\partial z = 192$ T m⁻¹. Note the small deflection for Mn₁₉ compared to Mn₁₈ and Mn₂₀.

is a result of the deflection of the clusters toward high field. This high field-seeking behavior has been also observed in molecular beam studies of Fe_{*n*} [18,21,22], Co_{*n*} [22–24], Ni_{*n*} [18,22,25,26], and Rh_{*n*} [1,2], and is consistent with superparamagnetism, whereby the overall magnetic moment of the *n* atom cluster μ_{cluster} is determined by the ferromagnetic coupling of spins. For ideal ferromagnetic coupling, $S_{\text{cluster}} = nS_{\text{atom}}$ and, hence, $\mu_{\text{cluster}} = n\mu_{\text{atom}}$ [27]. In the presence of a magnetic field rapid, thermally induced fluctuations in the direction of the cluster magnetic moment accompany spin relaxation among the $2S_{\text{cluster}} + 1$ magnetic sublevels, reducing the magnetization $\langle M_z \rangle$ of the cluster ensemble. At temperatures in which $\mu_{\text{cluster}}B \ll kT$, as is the case in this and similar molecular beam experiments, the Langevin theory of the temperature dependence of paramagnetism predicts that magnetization $\langle M_z \rangle$ varies quadratically with the cluster magnetic moment (Curie's law): $\langle M_z \rangle = \mu_{\text{cluster}}^2 B/3kT = n^2 \mu_{\text{atom}}^2 B/3kT$ [28]. This expression is appropriate for situations in which the various anisotropy energies are negligible compared to kT , and has been used to analyze magnetic deflection measurements of transition metal clusters produced under conditions where its validity applies [18,19,29].

The magnetic moments per atom, μ_{atom} , determined for Mn₁₁–99 using the Curie's law expression given above, are plotted in Fig. 2. (Low signal intensities prevented measurements on clusters smaller than Mn₁₁). Distinct local minima in μ_{atom} are observed for Mn₁₃ and Mn₁₉. The observation of anomalously low μ_{atom} values at $n = 13$ and 19 suggests an icosahedral growth sequence in this range, with minima in μ_{atom} occurring at the highly coordinated “closed shell” species: the 13 atom icosahedron and the 19 atom double icosahedron. However, because there is no structural information available from either experiment or theory for Mn clusters in the size range studied here, the suggestion of icosahedral structures is put forth only as a tentative guess.

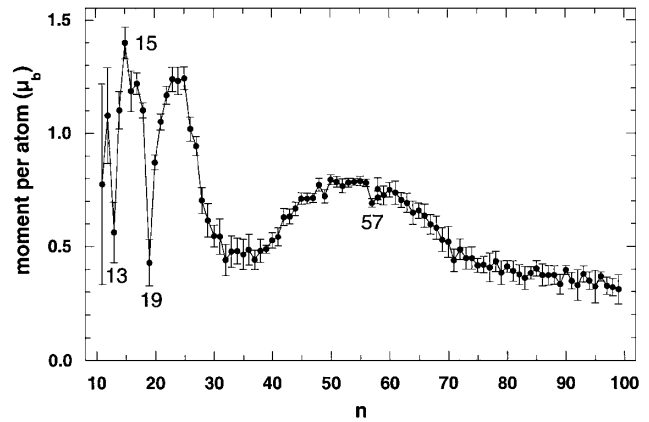


FIG. 2. Experimentally determined magnetic moments per atom, μ_{atom} , of Mn_{*n*}.

As shown in Fig. 2, the magnetic moments oscillate with increasing size, with a minimum observed around Mn_{32–37} and a local maximum at Mn_{47–56}. For a continuing icosahedral growth sequence and assuming, as above, that closed shell icosahedra display anomalously low μ_{atom} values, we would expect a local minimum to appear at Mn₅₅. However, as shown in Fig. 2, Mn₅₅ occurs near a local maximum in μ_{atom} . A small but distinct local minimum is observed at Mn₅₇. Beyond the indications of possible icosahedral structures for clusters having fewer than 20 atoms, there is no obvious structural/geometrical interpretation for the observed oscillatory size dependence in μ_{atom} . This is in contrast to the observed size dependence of nickel cluster magnetic moments, which exhibits minima in μ_{atom} at Ni₁₃, near Ni₅₅, and in the vicinity of other icosahedral shell or subshell closings [26].

First-principles calculations of the structures and magnetic properties of manganese clusters smaller than those studied here have predicted ferromagnetic ordering of atomic spins. Density functional theory (DFT) calculations performed by Nayak and Jena predict magnetic moments of $5\mu_b$ per atom for each cluster in the range Mn₂–Mn₅, independent of the basis set or of the specific functional used [6]. Calculations have been performed by Pederson *et al.* for Mn₂–Mn₈ using similar DFT methods [7]. These calculations produced the same overall geometries and magnetic moments as obtained by Nayak and Jena for Mn₂–Mn₅ except for the magnetic moment of Mn₅, which was predicted to be $4.6\mu_b$ per atom. Note that the theoretical predictions of ferromagnetic ordering in Mn₂ are at odds with the ESR studies of Weltner and co-workers, who determined this molecule to be a low-spin, antiferromagnetically ordered species [9]. The magnetic moments of Mn₆, Mn₇, and Mn₈ were calculated to be $4.33\mu_b$, $4.14\mu_b$, and $4.00\mu_b$ per atom, respectively [7]. The calculations predict that the smallest Mn clusters are characterized by van der Waals-like bonding, where the Mn atoms assume (to first order) a $3d^5 4s^2$ configuration, corresponding to a ${}^6S_{5/2}$ atomic

term and thus spin-only moments of $5\mu_b$ per atom, as found by detailed calculations. As cluster size increases, the average bond lengths trend downward toward the bulk (α Mn) value as minority-spin bonding states become populated, accompanied by a decrease in μ_{atom} .

Because the size range investigated in the present study does not overlap that of the calculations, direct comparison of theory and experiment is not possible. The maximum μ_{atom} value found in the present study was $\sim 1.4\mu_b$ (for Mn_{15}), well below the values calculated for the Mn_2 – Mn_8 . An upward trend in μ_{atom} with decreasing size is generally observed for those first-row transition metal clusters that display ferromagnetic ordering [2,22,26], and it is possible that the smaller manganese clusters may likewise display significantly higher μ_{atom} values. Efforts aimed at making these measurements are currently underway.

The author thanks Professor Lou Bloomfield and Professor Walt de Heer for informative discussions. This work is supported by the U.S. Department of Energy, Office of Basic Energy Sciences, Division of Chemical Sciences, under Contract No. W-31-109-ENG-38.

-
- [1] A. J. Cox, J. G. Louderback, and L. A. Bloomfield, *Phys. Rev. Lett.* **71**, 923 (1993).
- [2] A. J. Cox, J. G. Louderback, S. E. Apsel, and L. A. Bloomfield, *Phys. Rev. B* **49**, 12 295 (1994).
- [3] R. S. Trebble and D. J. Craik, *Magnetic Materials* (Wiley-Interscience, London, 1969).
- [4] D. C. Douglass, J. P. Bucher, and L. A. Bloomfield, *Phys. Rev. B* **45**, 6341 (1992).
- [5] L. A. Bloomfield, J. Deng, H. Zhang, and J. W. Emmert, in *Proceedings of the International Symposium on Cluster and Nanostructure Interfaces*, edited by P. Jena, S. N. Khanna, and B. K. Rao (World Scientific, Singapore, 2000).
- [6] S. K. Nayak and P. Jena, *Chem. Phys. Lett.* **289**, 473 (1998).
- [7] M. R. Pederson, F. Reuse, and S. N. Khanna, *Phys. Rev. B* **58**, 5632 (1998).
- [8] R. J. Van Zee, C. A. Baumann, S. V. Bhat, and W. Weltner, Jr., *J. Chem. Phys.* **76**, 5636 (1982).
- [9] C. A. Baumann, R. J. Van Zee, S. V. Bhat, and W. Weltner, Jr., *J. Chem. Phys.* **78**, 190 (1983).
- [10] J. R. Friedman, M. P. Sarachik, J. Tejada, and R. Ziolo, *Phys. Rev. Lett.* **76**, 3830 (1996).
- [11] H. Nagao, S. Yamanaka, M. Nishino, Y. Yoshioka, and K. Yamaguchi, *Chem. Phys. Lett.* **302**, 418 (1999).
- [12] M. R. Pederson and S. N. Khanna, *Chem. Phys. Lett.* **307**, 253 (1999).
- [13] A. Cornia, M. Affronte, A. G. M. Jansen, D. Gatteschi, A. Caneschi, and R. Sessoli, *Chem. Phys. Lett.* **322**, 477 (2000).
- [14] G. M. Koretsky and M. B. Knickelbein, *J. Chem. Phys.* **106**, 9810 (1997).
- [15] B. A. Collings, A. Amrein, D. M. Rayner, and P. A. Hackett, *J. Chem. Phys.* **99**, 4174 (1993).
- [16] D. McColm, *Rev. Sci. Instrum.* **37**, 1115 (1966).
- [17] W. A. de Heer and P. Milani, *Rev. Sci. Instrum.* **62**, 670 (1991).
- [18] J. A. Becker and W. A. de Heer, *Ber. Bunsen-Ges. Phys. Chem.* **96**, 1237 (1992).
- [19] J. P. Bucher and L. A. Bloomfield, *Int. J. Mod. Phys.* **7**, 1079 (1993).
- [20] M. B. Knickelbein (to be published).
- [21] W. A. de Heer, P. Milani, and A. Châtelain, *Phys. Rev. Lett.* **65**, 488 (1990).
- [22] I. M. L. Billas, A. Châtelain, and W. A. de Heer, *Science* **265**, 1682 (1994).
- [23] J. P. Bucher, D. C. Douglass, and L. A. Bloomfield, *Phys. Rev. Lett.* **66**, 3052 (1991).
- [24] D. C. Douglass, A. J. Cox, J. P. Bucher, and L. A. Bloomfield, *Phys. Rev. B* **47**, 12 874 (1993).
- [25] J. G. Louderback, A. J. Cox, L. J. Lising, D. C. Douglass, and L. A. Bloomfield, *Z. Phys. D* **26**, 301 (1993).
- [26] S. E. Apsel, J. W. Emmert, J. Deng, and L. A. Bloomfield, *Phys. Rev. Lett.* **76**, 1441 (1996).
- [27] S. N. Khanna and S. Linderoth, *Phys. Rev. Lett.* **67**, 742 (1991).
- [28] N. W. Ashcroft and M. D. Mermin, *Solid State Physics* (Saunders, Philadelphia, 1976).
- [29] A. Châtelain, *Philos. Mag.* **B 79**, 1367 (1999).